Supplementary Materials

1. Experimental

1.1. Materials and chemicals

Graphite (particle size < 20 μm), sulfuric acid (H_2SO_4, 98 %), phosphoric acid (H_3PO_4, 85 %), hydrogen peroxide (H_2O_2, 30 %), silver nitrate ($AgNO_3$), and ethanol (C_2H_5OH, 95 %) were purchased from Xilong Scientific Co. Ltd., China. All chemicals were used without further purification. The *A. paniculata* leaves were purchased in Ho Chi Minh City, Vietnam. Bacteria *Staphylococcus aureus* ATCC 25923, *Lactobacillus fermentum* ATCC 9338, *Escherichia coli* ATCC 25922, and *Pseudomonas aeruginosa* ATCC 27853 were purchased from Ho Chi Minh City Pasteur Institute, Vietnam. Nutrient broth and nutrient agar were purchased from Titan Biotech Ltd., India.

1.2. Extraction of *A. paniculata* leaves

The purchased *A. paniculata* leaves were initially rinsed and dried at 60°C, before being ground to collect leaf powder. 50 g of the powder was added to 500 mL of a mixture containing distilled water and ethanol. After that, the solution was heated to 90°C for 30 min, then vacuum filtered, and the obtained extract was centrifuged to remove any remaining residues. Subsequently, the *A. paniculata* extract was acquired and stored in the fridge.

1.3. Graphene oxide (GO) preparation

Graphene oxide (GO) was synthesized following our previous studies via the improved Hummers' method by using graphite as a precursor [1]. In the first step, 3 g of graphite powder was slowly added to the mixture including 360 mL of H_2SO_4 and 40 mL of H_3PO_4 under constant stirring at a temperature of less than 20°C. Following that, 18 g of $KMnO_4$ was gradually added to the solution while a relatively low temperature remained, as well. The mixture was then stirred at 50°C for 12 h, and continuously adding 500 mL of distilled water was, afterward, the addition of 15 mL of H_2O_2 solution. Subsequently, the product was centrifuged and washed with distilled water several times before being dried at 60°C for 24 h to obtain solid graphite oxide (GiO). The obtained GiO was dispersed in distilled water to achieve a concentration of 5 mg/mL. Finally, after another 12 h of ultrasonication treatment, the GO suspension was obtained.

1.4. Characterization of materials

Fourier-transform infrared spectroscopy (FTIR) (Alpha-E, Bruker Optik GmbH, Ettlingen, Germany) was utilized to identify the functional groups at wavenumber in the range of 4000 to 500 cm^{-1}. X-ray diffraction (XRD) was used to observe the structure of materials by CuKα radiation (λ = 0.154 nm) in the scope of 5~80 ° (D2 Phaser, Brucker, Germany). Raman spectra were recorded using a LabRam micro-Raman system at an excitation wavelength of 632 nm (He-Ne laser). Energy-dispersive X-ray spectroscopy (EDS) (Jeol-JMS 6490, Japan) was performed at an accelerating voltage in a range of 0 − 3.5 kV. Field emission-scanning electron microscope (FE-SEM) images (Hitachi S-4800, Japan) was conducted to observe the morphology and size of samples. The colloidal stability was determined using the Zeta potential by dynamic light scattering (DLS, Zetasizer Nano ZS from Malvern Instruments, Malvern, UK) at 25°C.

In addition, the electrochemical properties of samples were evaluated using CV and EIS. Particularly, the fabricated samples were mixed with carbon black and dispersed into ethanol. The obtained suspension was then coated onto the glassy carbon electrode, which acted as a working electron in a standard three-electrode glass cell of a CH Instrument 760D electrochemical workstation. Besides, a Pt wire and a calomel electrode were used as a counter and reference electrode, respectively.

1.5. Bioactivities

The antibacterial activities of AgNPs@GO were investigated against the Gram-positive (*S. aureus* and *L. fermentum*) and Gram-negative (*E. coli* and *P. aeruginosa*) bacteria strains using the optical density method. Bacteria were pre-cultured in the nutrient medium with a concentration of 10^6 CFU/mL, then, the sample was added and incubated at 37°C for 24 h. The concentrations of the sample were investigated at 100, 25, 12.5, and 6.25 µg/mL. Subsequently, the optical density at 600 nm (OD600) was monitored via UV-Vis spectra and the inhibition rate (H, %) was consequently calculated using Equation (S1):

$$H\ (\%)\ =\ \frac{OD_{test} - OD_{positive}}{OD_{negative} - OD_{positive}} \tag{S1}$$

where $OD_{negative}$, $OD_{positive}$, and OD_{test} were the absorbance of the negative control (distilled water), the positive control (antibiotics), and the test sample, respectively.

Besides, the antibacterial performance of the extract, Ag@GO composite, AgNPs, and GO as compared to the negative control (distilled water) and positive one (tetracycline) was evaluated using the inhibition zone method. At first, the sample was dispersed in deionized water at 100 µg/mL of concentration. Then, 20 µL of the obtained suspension was then dropped onto the filter paper in a Petri dish (~5 mm in diameter). Finally, the sample was incubated at 37°C for 24 h and then the inhibition zone diameter was recorded.

The cytotoxicity test of AgNPs@GO was determined towards the cancerous KB and the normal HEK-293 cell lines throughout the 3-(4,5-dimethylthiazol-2-yl)-2,5-diphenyltetrazolium bromide (MTT) assay. Cells activated were maintained in Dulbecco's Modified Eagle Medium (DMEM) culture media and kept in culture flasks at 37°C and 5% CO_2 for 2 – 3 days. As detail description, at first, 190 µL of cells were seeded into a 96-well plate at a density of 3×10^4 cells/well before being treated with 10 µL of culture medium containing tested samples at different concentrations (100, 50, 25, 12.5, and 6.25 µg/mL), followed by incubation at 37°C for 72 h. After 24 h of incubation, the culture medium was replaced with a fresh medium. After that, the treated cells were fixed by adding 10 µL of MTT working solution, which was 5 mg/mL in phosphate buffer solution to each well, and the plate was incubated for 4 h at 37°C in a CO_2 incubator. The medium was subsequently removed, and the formed formazan crystals were solubilized by adding 100 µL of dimethyl sulfoxide (DMSO) per well. Finally, the intensity of the dissolved formazan crystals with purple color was quantified using the enzyme-linked immunoabsorbent assay (ELISA) plate reader at 540 nm. The tests were performed on cell lines of KB and HEK-293. The effects on the cell rate (I_{MTT}, %) were calculated according to Equation (S2) below:

$$\text{IMTT (\%)} = \frac{A_0 - A}{A_0} \times 100 \qquad (S2)$$

where A_0 is the optical density of the initial sample and A is the optical density of the examined sample.

1.6. Electrochemical detection of H_2O_2

Electrochemical tests were performed at room temperature using a potentiostat/galvanostat CompactStat (Ivium Technologies, The Netherlands). All electrochemical measurements were run in the three-electrode system wherein a platinum wire, Ag/AgCl, and bare or Ag@GO (diameter of 3.0 mm) served as the counter, reference, and working electrodes respectively. Electrode characterization was performed using cyclic voltammetry (CV). The CV curves were recorded in the potential range of −0.5 to +0.5 V (vs Ag/AgCl) and at a scan rate of 100 mV s^{-1} in 0.1 M phosphate buffer solution (PBS) at a pH of 7.2. The influence of H_2O_2 was also measured in 0.1 M PBS (pH = 7.2) in the scan rate range of 25 to 175 mV s^{-1} within a separate range of concentration such as $0 - 15$ μM and $60 - 180$ μM. All experiments were carried out at room temperature.
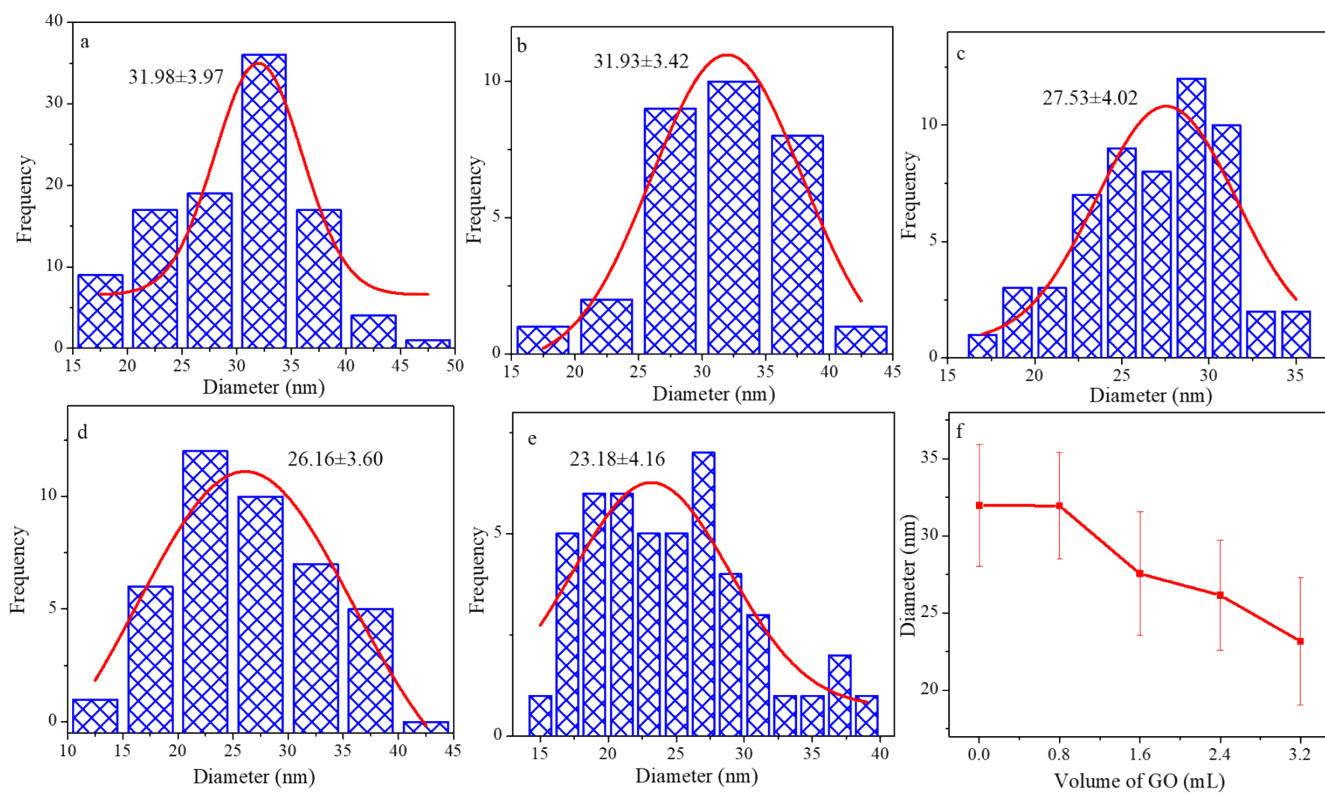
2. Results and discussion
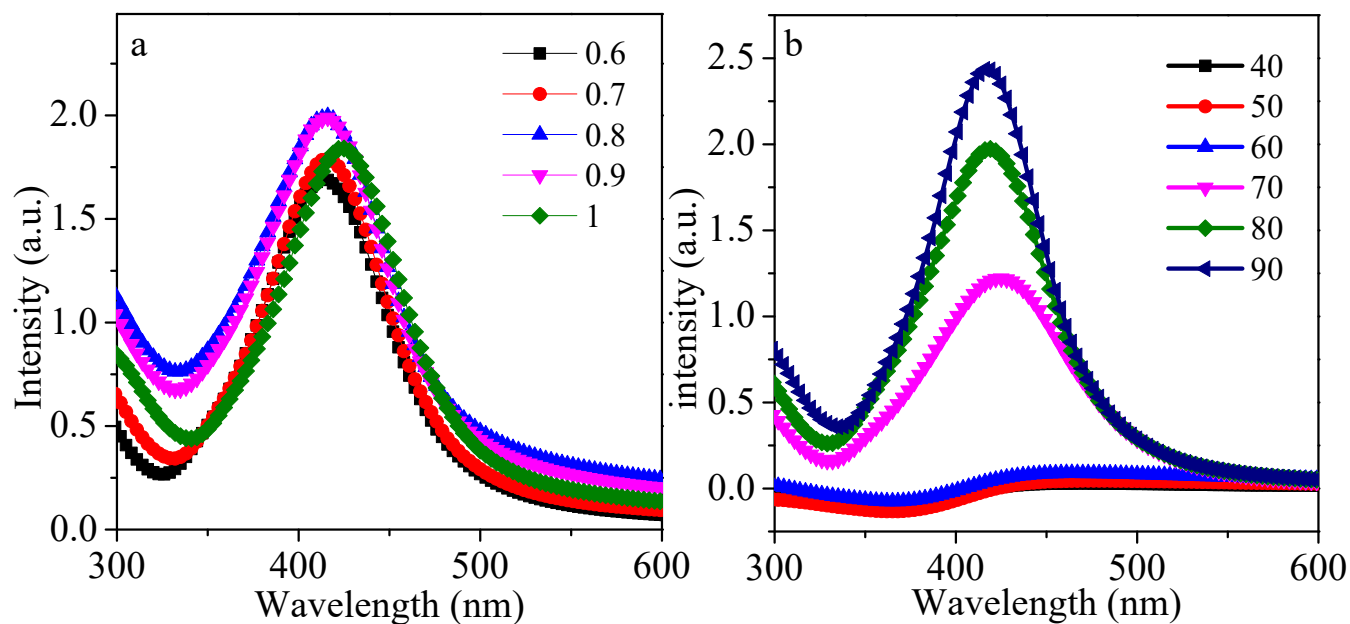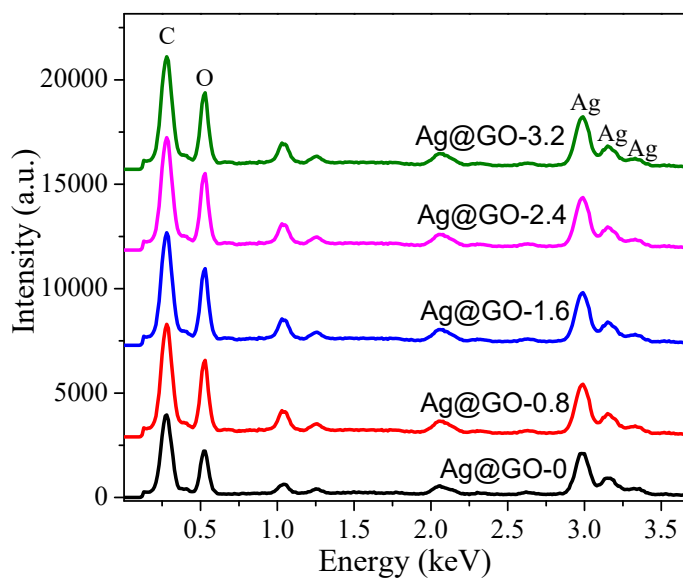

Figure S1. Effect of (a) AgNO$_3$ volume (mL)* and (b) temperature (°C)** on the formation of AgNPs

*1 mL of extract, 1 mL of pH 10 buffer solution, 80°C
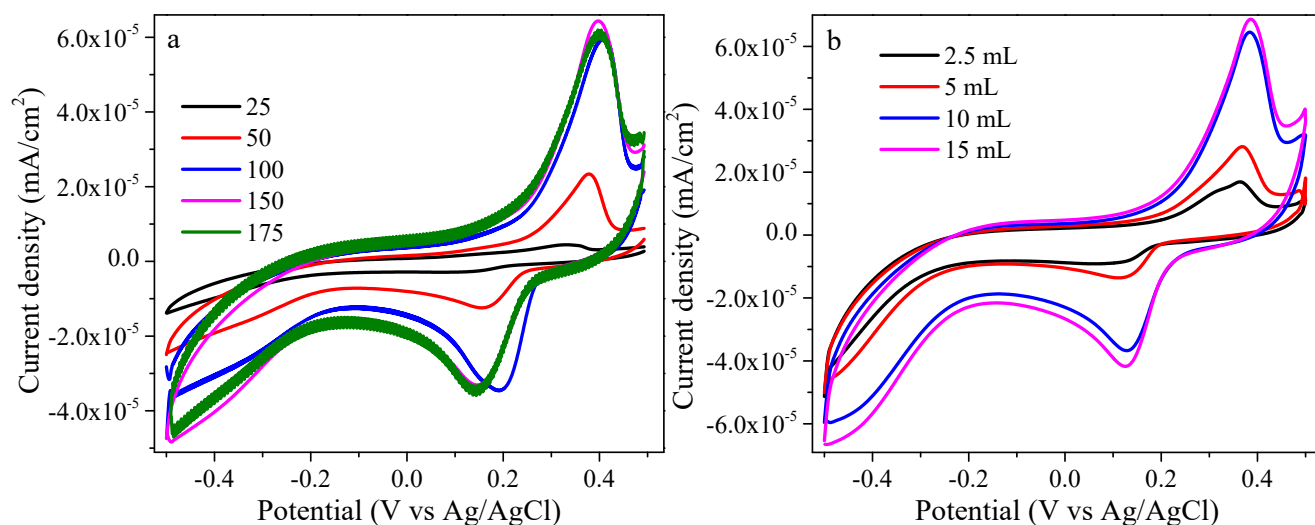
**1 mL of extract, 1 mL of pH 10 buffer solution, 0.8 mL of AgNO$_3$ 5 g/L

Figure S2. Particle size distribution graphs of Ag@GO synthesized at different GO volumes (0, 0.8, 1.6, 2.4, and 3.2 mL)

Figure S3. EDS spectra and elemental composition of AgNPs@GO samples

Figure S4. Effects of (a) scan rate and (b) material volume on the CV curve
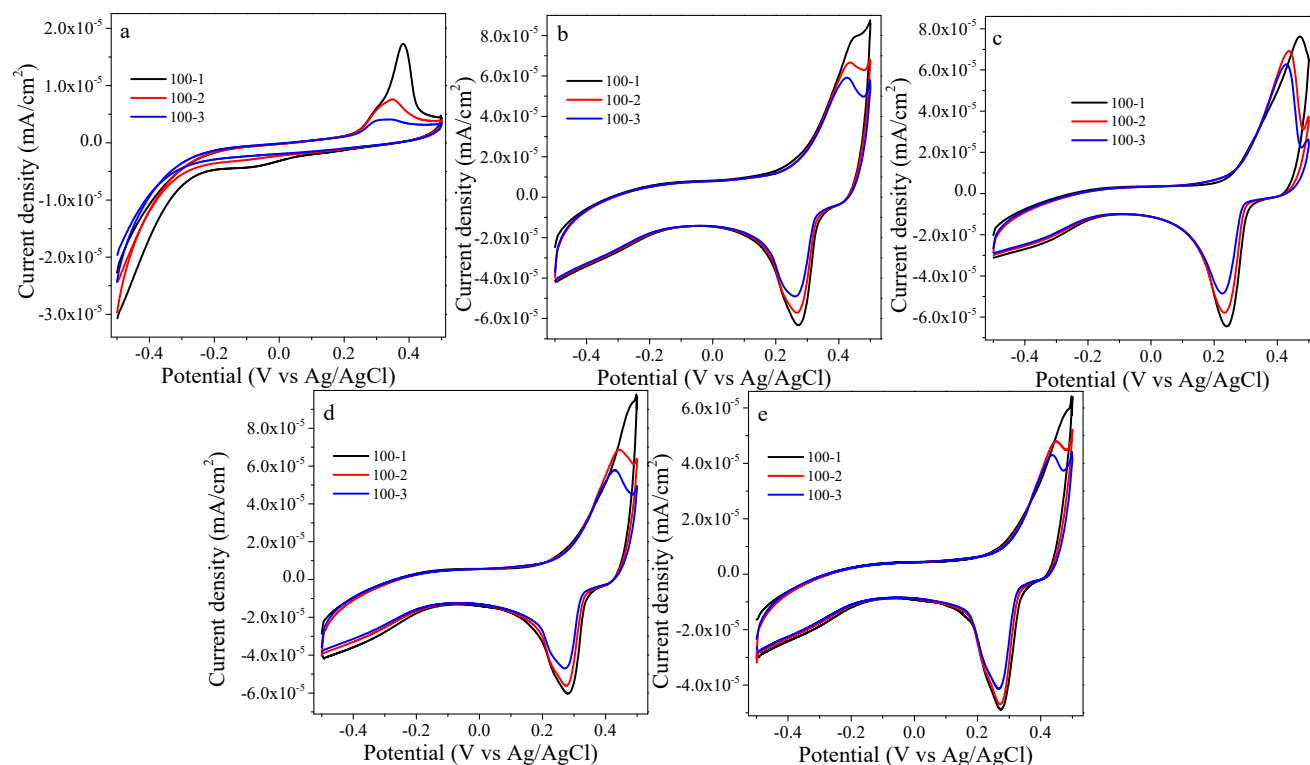
Figure S5. CV curve of AgNPs with different GO volumes of (a) 0, (b) 0.8, (c) 1.6, (d) 2.4, (e) 3.2 mL GO
(scan rate of 100 mV/s with three cycles)

Table S1. Elemental mass percentage of Ag@GO samples

Samples	Ag	C	O	Other elements (Na, Mg, S)
Ag@GO-0	61.45 ± 0.5	18.53 ± 0.06	16.3 ± 0.14	3.72 ± 0.08

Ag@GO-0.8	55.40 ± 0.42	19.61 ± 0.06	19.65 ± 0.14	5.34 ± 0.10
Ag@GO-1.6	49.81 ± 0.39	20.95 ± 0.06	24.07 ± 0.14	5.17 ± 0.09
Ag@GO-2.4	43.32 ± 0.39	22.96 ± 0.07	25.85 ± 0.16	7.87 ± 0.21
Ag@GO-3.2	38.05 ± 0.32	29.94 ± 0.07	26.98 ± 0.14	5.03 ± 0.09

Table S2. Antibacterial efficiency of materials containing AgNPs

No.	Samples	Reducing agent	Microbial strain	Concentration	Inhibition efficiency (%)	References
1	Ag@GO-1.6	A. paniculata extract	P. aeruginosa	100 µg/mL	94	This work
			E. coli		88	
			S. aureus		79	
			L. fermentum		71	
2	AgGO	glucose	S. aureus	100 µg/mL	~0	[2]
			S. epidermidis			
3	AgNPs@HTCS	–	S.aureus, E.coli	0.25 g/L	99	[3]
4	CEAgNP	DMF	S.aureus, E.coli	–	~100	[4]
5	AgNPs	the cell-free beef extract	S.aureus	50 µg/mL	96.7	[5]
			E.coli		97.5	
6	AgNPs@Se-CHAP/PCL	nanosecond laser system	S.aureus	2 mg/mL	43	[6]
			E.coli		45	
7	Ch-AgNPs	NaBH$_4$	P. aeruginosa	100 µg/mL	95	[7]
			S.aureus		85	
8	AgNPsT	T. serpyllum		2.5 µg/mL		[8]
	AgNPsS	S. officinalis	S. aureus, E. coli	3 µg/mL	20 – 40	
	AgNPsJ	T. pratense		6 µg/mL		

Table S3. Electrochemical detection efficiency of materials containing AgNPs

No.	Sample	Linear range (mM)	LOD (µM)	Reference
1	Ag@GO-1.6	0 – 0.015	2.65	This work
		0.06 – 0.18	29.23	
2	[Co(pbda)(4,4-	0.05 – 9	3.76	[9]

	bpy)(2H$_2$O)]n/GCE			
3	Cu-MOF/MPC/GCE	0.01 − 11.6	3.2	[10]
4	Co$_3$O$_4$/MWCNTs/CPE	0.02 − 0.43	2.46	[11]
5	AgNPs/3DG	0.03 − 16.21	14.9	[12]
6	PQ11-Ag NPs/GCE	0.1 − 180	33.9	[13]
8	Ag/Cu$_2$O/GCE	0.002 − 13.0	0.7	[14]
9	Ag-graphene-GC	0.1 − 40	28	[15]
10	Ag NPs-NFs/GCE	0.1 − 80	62	[16]

References

[1]   N.M. Dat, C.Q. Cong, N.D. Hai, L.M. Huong, N.T.H. Nam, D.Q. Tinh, L.T. Tai, H. An, M.Q. Duy, M.T. Phong, N.H. Hieu, Facile Synthesis of Eco-Friendly Silver@Graphene Oxide Nanocomposite for Optical Sensing, ChemistrySelect. 8 (2023). https://doi.org/10.1002/slct.202204183.

[2]   S.W. Chook, C.H. Chia, S. Zakaria, M.K. Ayob, K.L. Chee, N.M. Huang, H.M. Neoh, H.N. Lim, R. Jamal, R. Rahman, Antibacterial performance of Ag nanoparticles and AgGO nanocomposites prepared via rapid microwave-assisted synthesis method, Nanoscale Research Letters. 7 (2012) 1–7.

[3]   Z. Liu, L. Wang, X. Zhao, Y. Luo, K. Zheng, M. Wu, Highly effective antibacterial AgNPs@ hinokitiol grafted chitosan for construction of durable antibacterial fabrics, International Journal of Biological Macromolecules. 209 (2022) 963–971.

[4]   A.W. Jatoi, I.S. Kim, Q.Q. Ni, A comparative study on synthesis of AgNPs on cellulose nanofibers by thermal treatment and DMF for antibacterial activities, Materials Science and Engineering: C. 98 (2019) 1179–1195.

[5]   G. Ghodake, M. Kim, J.-S. Sung, S. Shinde, J. Yang, K. Hwang, D.-Y. Kim, Extracellular synthesis and characterization of silver nanoparticles—Antibacterial activity against multidrug-resistant bacterial strains, Nanomaterials. 10 (2020) 360.

[6]   A.A. Menazea, S.A. Abdelbadie, M.K. Ahmed, Manipulation of AgNPs coated on selenium/carbonated hydroxyapatite/ε-polycaprolactone nano-fibrous via pulsed laser deposition for wound healing applications, Applied Surface Science. 508 (2020) 145299.

[7]   A. Parthasarathy, S. Vijayakumar, B. Malaikozhundan, M.P. Thangaraj, P. Ekambaram, T. Murugan, P. Velusamy, P. Anbu, B. Vaseeharan, Chitosan-coated silver nanoparticles promoted antibacterial, antibiofilm, wound-healing of murine macrophages and antiproliferation of human breast cancer MCF 7 cells, Polymer Testing. 90 (2020) 106675.

[8]   K. Sehnal, M. Gargulak, A.E. Ofomaja, M. Stankova, B. Hosnedlova, C. Fernandez, M. Docekalova, J.

Sochor, M. Kepinska, Z. Tothova, Biophysical analysis of silver nanoparticles prepared by green synthesis and their use for 3D printing of antibacterial material for health care, in: 2019 IEEE International Conference on Sensors and Nanotechnology, IEEE, 2019: pp. 1–4.

[9]   L. Yang, C. Xu, W. Ye, W. Liu, An electrochemical sensor for H2O2 based on a new Co-metal-organic framework modified electrode, Sensors and Actuators B: Chemical. 215 (2015) 489–496.

[10]   Y. Zhang, X. Bo, C. Luhana, H. Wang, M. Li, L. Guo, Facile synthesis of a Cu-based MOF confined in macroporous carbon hybrid material with enhanced electrocatalytic ability, Chemical Communications. 49 (2013) 6885–6887.

[11]   H. Heli, J. Pishahang, Cobalt oxide nanoparticles anchored to multiwalled carbon nanotubes: synthesis and application for enhanced electrocatalytic reaction and highly sensitive nonenzymatic detection of hydrogen peroxide, Electrochimica Acta. 123 (2014) 518–526.

[12]   B. Zhan, C. Liu, H. Shi, C. Li, L. Wang, W. Huang, X. Dong, A hydrogen peroxide electrochemical sensor based on silver nanoparticles decorated three-dimensional graphene, Applied Physics Letters. 104 (2014) 243704.

[13]   W. Lu, G. Chang, Y. Luo, F. Liao, X. Sun, Method for effective immobilization of Ag nanoparticles/graphene oxide composites on single-stranded DNA modified gold electrode for enzymeless H2O2 detection, Journal of Materials Science. 46 (2011) 5260–5266.

[14]   C. Qi, J. Zheng, Novel nonenzymatic hydrogen peroxide sensor based on Fe3O4/PPy/Ag nanocomposites, Journal of Electroanalytical Chemistry. 747 (2015) 53–58.

[15]   S. Liu, J. Tian, L. Wang, H. Li, Y. Zhang, X. Sun, Stable aqueous dispersion of graphene nanosheets: noncovalent functionalization by a polymeric reducing agent and their subsequent decoration with Ag nanoparticles for enzymeless hydrogen peroxide detection, Macromolecules. 43 (2010) 10078–10083.

[16]   J. Tian, S. Liu, X. Sun, Supramolecular microfibrils of o-phenylenediamine dimers: oxidation-induced morphology change and the spontaneous formation of Ag nanoparticle decorated nanofibers, Langmuir. 26 (2010) 15112–15116.